

Study of Fuel Staging for NOx Control in an Oil-fired Furnace

S. R. Wu¹, H.S. Shim², B. R. Adams² and S. L. Chen³

¹ Energy & Resources Labs, Industrial Technology Research Institute
Bldg. 64, 195 Sec. 4, Chung Hsing Rd.
Chutung, Hsinchu, Taiwan 310, R.O.C.

² Reaction Engineering International
77 West 200 South, Suite 210
Salt Lake City, Utah 84101, USA

³ Pacific Rim Technologies
50 Ln 46 Ave 688, Jong Jeng Rd.
Pingtung, Taiwan 900, R.O.C.

Abstract

This paper summarizes the design of burner systems with CFD simulations to identify effective designs for NOx control in an oil-fired furnace with 1200 preheated combustion air. The study focused on the design of fuel staging systems. However, air staging was also conducted as a basis for comparison. Simulation results indicate that fuel staging was more effective than air staging to control the NOx formation in the furnace. The NOx produced with air staging, 1258 ppm, was reduced to 782 ppm with fuel staging. For fuel staging, the formation of NOx in the furnace was found to be more strongly dependent on the location of the fuel injector and the injection angle than on the fuel spray angle. A successful fuel-staging configuration was identified and simulated to produce 199 ppm of NOx at the furnace exit. Examination of the fuel distribution profiles in the furnace suggests that the delayed mixing between the oil droplets and the preheated air was the key to low NOx formation.

1 Introduction

The Energy & Resources Laboratories of Industrial Technology Research Institute (ERL-ITRI) has developed a 1,000,000 kcal/hr oil-fired furnace to evaluate the operation and performance of an oil-fired regenerative combustion system based on the High Cycle Regenerative Combustion System (HRS) concept described by Nippon Furnace for gas-fired furnaces [1]. As part of the furnace operation and performance evaluations, ITRI utilized CFD simulations to understand the effects of different burner designs on temperature distributions and CO and NOx emissions prior to burner constructions.

Previous studies indicated that air staging was not effective in reducing NOx formation given the burner design in this furnace [2]. This paper reviews the modelling investigation of fuel staging as a strategy for NOx reduction. The study focuses on oil injection configurations, oil droplet trajectories and vaporization, gas flow patterns, heat transfer and NOx formation in the furnace. The computer model used for this study was a CFD-based reacting flow code, *GLACIER*, developed by Reaction Engineering International (REI).

2 Model Description

The REI *GLACIER* code employs a combination of Eulerian and Lagrangian reference frames [3-6] to solve the governing conservation equations. The flow field is assumed to be a steady-state, turbulent, reacting continuum field that can be described locally by general conservation equations. The governing equations for steady state, turbulent, gas-phase fluid mechanics, heat transfer, thermal radiation and scalar transport are solved in an Eulerian framework. The governing equations for droplet-phase mechanics and reactions are solved in a Lagrangian reference frame. Dispersion of the droplet cloud is based on statistics gathered from the turbulent flow field. The overall solution scheme is based on a particle-in-cell approach. The gas-phase mass, momentum and energy equations can be classified as Eulerian, steady-state, second-order, non-linear, elliptical, partial differential equations (PDE). The equations can be cast into a standard format to simplify the finite differencing structure. The standard form for the governing gas-phase equations in Cartesian coordinates may be written in Favre-averaged form as:

$$\frac{\partial(\bar{\rho}\bar{u}\phi)}{\partial x} + \frac{\partial(\bar{\rho}\bar{v}\phi)}{\partial y} + \frac{\partial(\bar{\rho}\bar{w}\phi)}{\partial z} - \frac{\partial}{\partial x}\left(\Gamma_{\phi}\frac{\partial\phi}{\partial x}\right) - \frac{\partial}{\partial y}\left(\Gamma_{\phi}\frac{\partial\phi}{\partial y}\right) - \frac{\partial}{\partial z}\left(\Gamma_{\phi}\frac{\partial\phi}{\partial z}\right) = S_{\phi}$$

where ϕ represents the scalar variable of interest (e.g., velocity, enthalpy, mixture fraction), Γ_{ϕ} and S_{ϕ} represent diffusion and an appropriate source term depending on the variable described, respectively [3]. The differential equation is integrated over each control volume. Piecewise profiles expressing the variation of ϕ (the scalar variable of interest) between the grid points are used to evaluate the required integrals. The result is the discretization equation containing the values of ϕ for a group of grid points [7]. Turbulence is modeled using the traditional two-equation k- ϵ model [8] due to its general applicability in modeling the mean velocity field in reacting flows.

The solution algorithm for two-phase flow employs a series of macro-iterative loops over the droplet and gas phase calculations. Within each gas phase macro-iteration loop, an iterative loop is performed over the governing PDE for fluid mechanics, enthalpy, "chemistry" (i.e., fuel stream mixture fractions and their variances), and radiative transport in a sequential manner to obtain updated solution values. The

discretized equations for the gas phase are solved using a pressure-based, segregated variable scheme developed for low speed, variable density flows (SIMPLER [7]). Gas properties are updated by first computing the local mean mixture fraction and parameterized heat loss variables, and then computing the local mean thermo-chemical properties of the gas based on chemical equilibrium assumptions. Within the model, the rate at which the primary combustion reactions occur is assumed to be limited by the rate of mixing between the fuel and the oxidizer, which is a reasonable assumption for the chemical reactions governing heat release. Then, the thermochemical state at each spatial position is a function of the degree of mixing, the mass fraction of oil off-gas, and the enthalpy. The effect of turbulence on the mean chemical composition is incorporated by assuming that the mixture fraction, obtained using the $k-\epsilon$ model, is described by a “clipped-Gaussian” probability density function having spatially varying mean and variance. Mean chemical species concentrations are obtained by convolution over this assumed probability density function (PDF). Chemical reactions that are kinetically controlled, such as those involved in the formation and destruction of nitrogen oxides (NO_x), are handled differently to account for the effects of their relatively slow reaction rates in comparison to the mixing rates. NO_x formation/destruction in the ITRI HRS furnace is modeled using a reduced mechanism developed by REI. The reduced mechanism approach used by REI is based on conventional reduced mechanism methods [9, 10]. This methodology uses the assumption that certain species contained within a complete detailed chemical mechanism are in steady state (i.e. their rate of production is equal to their rate of destruction). A list of finite rate NO-related species tracked in the REI’s reduced mechanism used in modeling the ITRI HRS furnace includes CO, OH, NO, N₂O, HNCO, NH₃, CO₂, O₂, H₂O, HCN, H₂, and N₂. The reference detailed mechanism used in the development of the reduced mechanism is the mechanism of Miller and Bowman [11] with literature modifications [12]. This detailed mechanism contains over 60 chemical species and 250 reversible elementary reactions [13]. This is a more rigorous and universal approach than curve-fitting type approaches which were used to generate simple global mechanisms [14]. The total number of transfer equations that must be solved within the CFD simulation is equal to the number of major non-steady state species. Historically, reduced mechanism methods have been difficult to use effectively due to the amount of human time necessary in deriving them. To overcome this difficulty, REI uses an approach that automates the reduction process called Computer Assisted Reduction Method (CARM), developed by Professor J. Y. Chen at the University of California, Berkeley [15]. REI’s use of the reduced mechanism approach and use of CARM is described in more detail elsewhere [14].

The droplet or particle phase is computed by solving an initial value problem for the mean trajectory and dispersion of the cloud of droplets. Included in the system of ordinary differential equations (ODEs) are equations for: droplet momentum, continuity of species, droplet energy and droplet liquid vaporization. The governing set of ODEs is solved using a time-accurate predictor-corrector method for stiff ODEs. Oil droplet reactions include droplet vaporization and gas-particle interchange. The droplet evaporation rate is based on the mass transfer between the vapor at the droplet surface (saturated vapor pressure) and the bulk gas. The droplet temperature is based on a droplet energy balance. Once the oil droplet reaches the boiling point, the droplet temperature remains at the boiling temperature until all liquid is vaporized

(at a rate determined by an energy balance on the droplet). The radiative intensity field and surface heat fluxes are calculated using the discrete ordinates method [16]. The discrete-ordinates method has been shown to be a viable choice for modeling radiation in combustion systems, both in terms of computational efficiency and accuracy. The development of the discrete-ordinates method and its application to a number of complex geometries have been presented in the literature and serve to validate the use of this method in accurately modeling radiative heat transfer in boilers [16, 17]. Effects of variable surface properties and participating media (gas, soot and droplets) are included.

Although the operation of the ITRI HRS furnace is inherently transient in nature, firing alternatively from each end of the furnace, it is feasible to use a steady state model to evaluate various NO_x emissions by different burner options for comparison purposes. The burner behavior will control the furnace NO_x and CO levels, thus characterizing the burner behavior under different designs will give an indication of how the NO_x, CO and temperature will change for the different designs. In the current modeling efforts, therefore, only steady state one-end firing was modelled.

3 Furnace and Burner

The ITRI test furnace is 8 m in length, 2 m in width, and 2 m in depth. Opposed burners are centered on each end wall. The furnace is refractory lined. Five cooling tubes are distributed over the floor of the furnace. Preheated air is fed to the furnace via an air plenum and a burner quarl as shown in Figure 1. For air staging, the oil was injected through an injector (F1) at the center of the burner quarl but angled at 30° with respect to the furnace axis as shown on the figure. The preheated combustion air was directed through four ports outside the burner quarl as shown on the top plot of Figure 1. For fuel staging, the oil was injected through two injectors (F2) located diagonally outside the burner quarl. The preheated combustion air was fed through the center of the burner quarl for all fuel staging configurations.

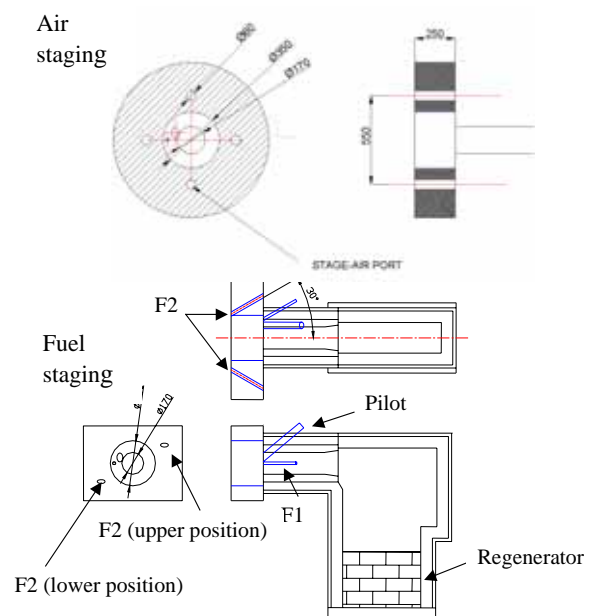


Figure 1. Regenerative-burner system.

The operating conditions modelled for the furnace were maintained constant over all tests at a stoichiometry of 1.23 and an exit O₂ of 4.2% (dry). The temperature and the flow rate of the combustion air were 1,222 °C and 1,192 Nm³/hr, respectively. The oil was injected at a flow rate of 87.6 liters/hr and a temperature of 110 °C. The oil contained 85.92% C, 12.35% H, 0.13% N, 0.93% S, 0.28% O, 0.05% ash, and 0.34% moisture. The heating value of the oil was 10,535 kcal/kg. The oil droplet size distribution for the model was based on extrapolation from 40 µm SMD water test results conducted with an effervescent atomizer at ITRI.

4 Results and Discussion

Table 1 summarizes the simulation results. They include one air staging configuration, Case A, and three fuel staging configurations, Case B, Case C, and Case D.

	Case A	Case B	Case C	Case D
Air injection location	4 ports	Center	Center	Center
Oil injector location	Center	Diagonal	Diagonal	Diagonal
Oil injection angle	30	30	0	0
Oil spray angle	45	45	25	45
Preheated combustion air,	1,222	1,222	1,222	1,222
Exit temp.,	1,384	1,369	1,365	1,365
Exit CO, ppm (wet)	56	51	52	53
NO _x , ppm (6% O ₂)	1,258	782	199	227

Table 1. Simulation Results

4.1 Air Staging

Air staging (Case A) produced a significant amount of NO_x (1,258 ppm) in the furnace as shown in Table 1. Although 59% of the combustion air was staged through the four ports outside the burner quarl, this was not sufficient to produce a fuel-rich core flow near the burner [2]. The staged air was interspersed with the oil droplets from the angled oil injector. As a result, a fraction of the droplets vaporized within the core flow whereas a larger fraction vaporized outside the core flow. Figure 2 shows distributions of the oil off-gas (vaporized oil) along the furnace for Case A (top plot). It can be seen that there exist numerous zones where fuel and air mix. These mixing zones resulted in high gas temperatures which promoted the observed high NO_x formation.

4.2 Fuel Staging

In an effort to minimize the area over which the oil off-gas (fuel) and high temperature air mix, a fuel-staging configuration, Case B, was designed and modelled. In this case, the combustion air entered through the core and the oil was injected through two injectors outside the burner quarl. The oil injection angle and the spray angle remained the same at 30° and 45°, respectively, as in the air staging case. As shown on the middle plot of Figure 2, there were more fuel-rich than fuel-lean mixing zones compared with the air staging case. Thus, less NO_x (782 ppm) was formed. Less intensive fuel-air contacting also reduced the furnace exit temperature from 1,384 °C to 1,369 °C. However, the exit CO concentration remained low at 51 ppm.

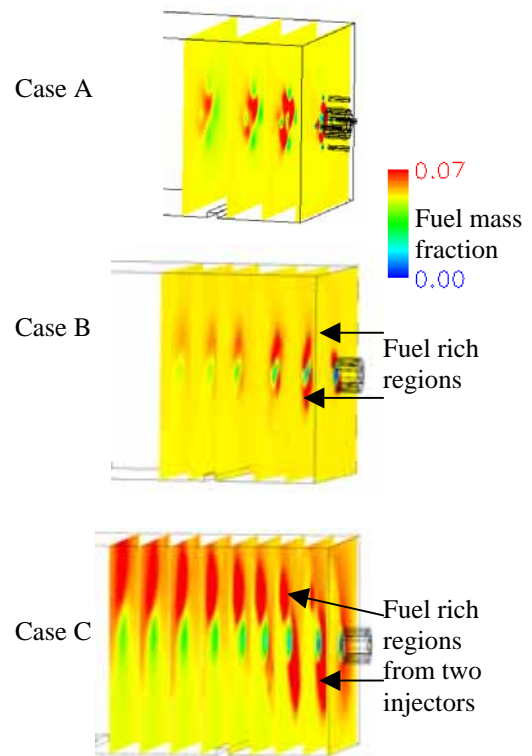


Figure 2. Comparisons of oil off-gas distribution.

4.3 Injector Location and Position

Examination of the oil droplets trajectories shown in Figure 3 (top plot) indicates that the two oil injectors (Case B) sprayed oil droplets rapidly into the core air stream near the burner due to their close proximity to the burner quarl and their off-axis injection angle. Therefore, for Case C, the injectors were moved a greater distance away from the burner quarl (~0.65 m from burner centerline) and the injectors were positioned parallel to the furnace axis (i.e., 0° injection angle). In addition, the oil spray angle was reduced from 45° to 25°. As indicated in Table 1, Case C provided the most effective approach to reducing NO_x formation in the furnace. The exit NO_x level of 199 ppm was about 75% lower than Case B. In general Case C allowed the oil off-gas (fuel) and the preheated core air to mix with the flue gas before mixing with each other (see off-gas profiles in the bottom plot of Figure 2), leading to less area with high-temperature fuel-air mixing zones and lower NO_x formation. Although local temperatures were lower due to less direct fuel-air mixing, overall furnace exit temperature and CO were similar to Case B because the furnace length allowed the fuel and air reactions to reach completion before the exit.

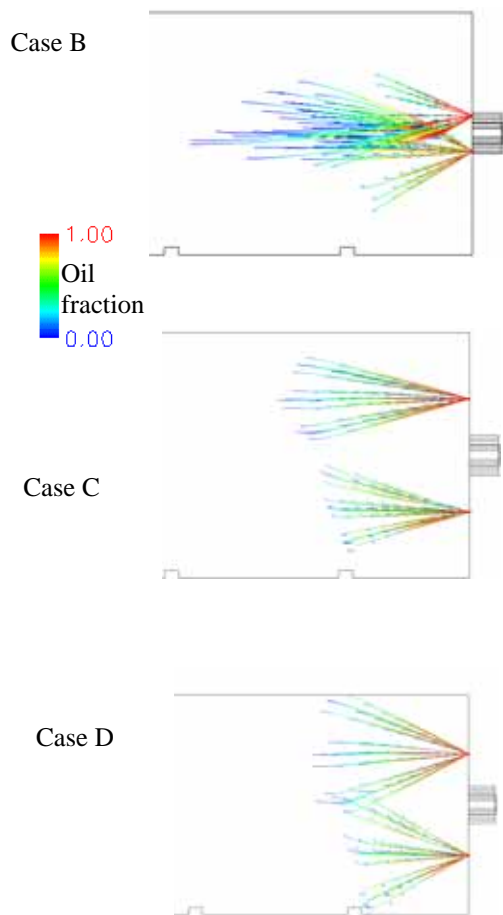


Figure 3. Oil droplet trajectories

4.4 Impacts of Spray Angle

Case D varied the oil injection spray angle to determine how much NO_x reduction observed in Case C could be attributed to the reduction of the oil spray angle versus the relocation of the oil injectors. There were also some concerns that a 25° spray angle might be too narrow to be manufactured. Case D was conducted with a spray angle of 45°. The rest of the conditions were identical to Case C. As shown in Figure 3, a wider spray angle allowed droplets to mix earlier with the preheated air near the burner. As indicated in Table 1, slightly higher NO_x was obtained. However, this amounts to only 14% increase (199 ppm to 227 ppm) from Case C. It is believed that the majority of the NO_x reduction observed in Case C was due to the more favorable injector location and position (injection angle).

5 Conclusions

The results of this study conclude that fuel staging was more effective than air staging to reduce NO_x formation in this furnace. The impacts of the fuel injector location, the injection angle and the spray angle were investigated with CFD simulations. Simulation results indicate that NO_x formation was more strongly dependent on the fuel injector location and the injection angle than on the spray angle. Examination of the predicted oil off-gas distribution in the furnace suggests that minimization of direct mixing between oil off-gas and preheated air minimized NO_x formation. It is believed that forcing the oil droplets and the preheated air to mix with furnace flue gas before mixing with each other is the key to

successful NO_x control. CFD simulations provide valuable guidance for the design of fuel staging systems.

6 Acknowledgments

For financial support, we thank the Bureau of Energy of Republic of China for research grants 92-D0220.

References

- [1] Hasegawa, T., Tanaka, R. and Kishimoto, K., High Temperature Excess-enthalpy Combustion for High Efficiency Improvement and NO_x Abatement, *Pacific Rim International Conference of AFRC/JFRC*, Maui, Hawaii 1994.
- [2] Adams, B.R., Shim, H.S., Wu, S.R., Chang, W.C., Chiao, J. and Chen, S.L., CFD Evaluation of NO_x Reduction Strategies in an Oil-fired Furnace, *4th Asia-Pacific Conference on Combustion*, Nanjing, P.R. China, 2003.
- [3] Smoot, L.D. and Smith, P.J., *Coal Combustion and Gasification*, Plenum Press, NY, 1985.
- [4] Jain, S., Three-Dimensional Simulation of Turbulent Particle Dispersion Applications, *Ph.D. Dissertation*, Department of Chemical and Fuels Engineering, University of Utah, 1998.
- [5] Baxter, L.L., Turbulent Transport of Particles, *Ph.D. Dissertation*, Department of Chemical Engineering, Brigham Young University, 1996.
- [6] Baxter, L.L., Bockelie, M.J., Adams, B.R., Cremer, M.A., Davis, K.A., Eddings, E.G., Valentine, J.R., Smith, P.J., Heap, M.P., *Computational Simulations of Industrial Furnaces, Computational Technologies for Fluid/Thermal/Chemical Systems with Industrial Applications*, San Diego, California, 1998.
- [7] Patankar, S.V., *Numerical Heat Transfer and Fluid Flow, Computational Methods in Mechanics and Thermal Sciences*, Hemisphere Publishing Corp., Washington D.C., 1980.
- [8] Launder, B.E., and Spalding, D.B., *Mathematical Models of Turbulence*, Academic Press, London, England, 1972.
- [9] Smooke, M.D. (Ed.), *Reduced Kinetic Mechanisms and Asymptotic Approximations for Methane-Air Flames*, Springer, 1991.
- [10] Peters, N. and Rogg, B. (Eds.) *Reduced Kinetic Mechanisms for Applications in Combustion Systems*, Springer, 1993.
- [11] Miller, J.A. and Bowman, C.T., *Prog. Energy Combust. Sci.* 15:287-338, 1991.
- [12] Dean, A.J., Hanson, R.K., and Bowman, C.T., *J. Phys. Chem.* 95:3180-3189, 1991.
- [13] Bockelie, M., *Reaction Engineering International*, Salt Lake City, UT, <http://www.reaction-eng.com/>
- [14] Cremer, M.A., Montgomery, C.J., Wang, D.H., Heap, M. P., Chen, J.-Y., *Proc. Combust. Inst.* 28:2427-2434, 2000.
- [15] Chen, J.-Y., *Combust. Sci. and Tech.* 57:89-94, 1988.
- [16] Adams, B.R. and Smith, P.J., Three-dimensional Discrete-ordinates Modeling of Radiative Transfer in a Geometrically Complex Furnace, *Comb. Sci. and Tech.* 88:293-308, 1993.
- [17] Adams, B.R. and Smith, P.J., Modeling Effects of Soot and Turbulence-Radiation Coupling on Radiative Transfer in Turbulent Gaseous Combustion, *Comb. Sci. and Tech.* 109:121-140, 1995.